Visual Abstract

Fatigue life investigation of notched TC4 specimens subjected to different patterns of laser shock peening

M. Zhelnin, A. Kostina, A. Iziumova, A. Vshivkov, E. Gachegova, O. Plekhov
Institute of Continuous Media Mechanics of the Ural Branch of Russian Academy of Science (ICMM UB RAS), Russia
zhelnin.m@icmm.ru, https://orcid.org/0000-0002-5721-3301
kostina@icmm.ru, https://orcid.org/0000-0002-5721-3301
fedorova@icmm.ru, https://orcid.org/0000-0002-1769-9175
vshivkov.a@icmm.ru, http://orcid.org/0000-0002-7667-455X
gachegova.e@icmm.ru, https://orcid.org/0000-0001-6849-9889
poa@icmm.ru, https://orcid.org/0000-0002-0378-8249

S. Swaroop
Vellore Institute of Technology, India
n.r.sathya.swaroop@gmail.com, https://orcid.org/0000-0001-9872-811X

ABSTRACT. The exhaustion of constructive ways for increasing the service life of parts has led to the development of new methods which can improve their material properties during operation under various loading conditions. Laser shock peening (LSP) induces compressive residual stress field which prevents fatigue crack initiation and propagation in components. Characteristics of laser impact and treatment patterns play an important role in efficiency of LSP application for improvement of fatigue properties. This work is devoted to the experimental examination of two LSP patterns to reveal the most optimal scheme from fatigue live improvement point of view. Proposed LSP pattern allowed one to increase the fatigue life of specimens with semi-circular notch by an order of magnitude. The numerical simulation of the LSP was performed to visualize the residual stress field of treated specimen after loading and to give the interpretation of the experimentally observed improvement of fatigue life.

KEYWORDS. Laser shock peening, Fatigue life, titanium alloy TC4, Johnson-Cook plasticity model.

OPEN ACCESS

Citation: Zhelnin, M., Kostina, A., Iziumova, A., Vshivkov, A., Gachegova, E., Plekhov, O., Swaroop, S., Fatigue life investigation of notched TC4 specimens subjected to different patterns of laser shock peening, Frattura ed Integrità Strutturale,65 (2023) 100-111.

Received: 23.03.2023
Accepted: 14.05.2023
Online first: 15.05.2023
Published: 01.07.2023

INTRODUCTION

The key benefit of Laser Shock Peening (LSP) treatment is enhancement of fatigue properties in metallic materials. Therefore, it has been widely applied to commercial alloys used in aerospace industry (especially aluminum and titanium) to increase fatigue life of aircraft components and engineering structures weakened by stress concentrators. A. G. Sanchez et al. [1] studied the effect of LSP with and without protective coating on the fatigue performance of AA7075-T651 aluminum samples with pre-corroded pits in them. They found that generated residual stresses effectively suppress the influence of corrosion pits and improve fatigue life up to 160 000 cycles for LSP without coating and 80 000 cycles for LSP with coating. J. G. Pretorius et al. [2] simulated residual stresses due to LSP in fillet radii step region on a high-speed gas turbine engine shaft made of AISI 4340 steel and estimated fatigue life in Fe-safe software. The results demonstrated substantial improvement by 553% in the case of LSP. Ren et al. [3] studied the effect of double-sided LSP of a thin Ti-6Al-4V dog-bone specimen on fatigue properties in presence of foreign object damage. They obtained that double-sided LSP increases fatigue performance of the sample by the introduction of compressive residual stresses. Similar results were obtained by J.-M. Yang et al. [4]. They applied LSP to the open hole specimens made of 2024-T3 aluminum alloy. The obtained results have shown significant improvement in fatigue performance for the various notch configurations when both sides of the samples were treated simultaneously. Jan Kaufman et al. [5] performed corrosion fatigue tests on rectangular specimens made of AA5083 aluminum alloy. The specimens subjected to LSP without protective coating and fully submersed into the water have better improvement of fatigue life (+69%) than samples with protective coating in standard laminar flow conditions (+59%).

Several studies compared the effectiveness of LSP with traditional surface improvement techniques although not all of them showed that LSP has better performance. For instance, A. Clauer [6] compared the fatigue life of AA7075-T7351 notched specimens treated by LSP with shot-peened (SP) specimens. He obtained that LSP induces a higher increase in the number of cycles to failure than SP. However, in [7] it was found that for fretting fatigue tests of Ti–6Al–4V dog-bone specimen SP gives better results than LSP. At the same time, the authors obtained deeper compressive residual stresses in the case of LSP but with a lower magnitude. J. Epp and H.-W. Zoch [8] compared LSP with Water Jet Peening (WJP) and Shot Peening (SP) with regard to the microstructure, surface topography, residual stresses, and fatigue properties for gear teeth-like specimens made of case-hardened steel. They have found that LSP has minimal effect on surface topology while WJP induces surface damage. SP is characterized by the presence of the strong plastic deformation. Regarding the fatigue properties, SP shows the highest improvement (+37%), while LSP and WJP demonstrate lower results (+15% and +23% respectively). In terms of the residual stresses, LSP has shown the deepest penetration of the compressive residual stresses but the magnitude is lower than SP, which is in agreement with the results presented in [7].

In addition to these findings, some works presented an insignificant or even deteriorating influence of LSP on fatigue life. Abdul-Jabar H. Ali [9] reported minor improvement (up to 1.534 times) in the fatigue life of AA7075 aluminum alloy specimens treated with LSP which were tested at a constant amplitude stress range from $0.3\sigma_u$ up to $0.8\sigma_u$, where σ_u is the ultimate strength. G. Ivetic et al. [10] studied the effect of laser shots treatment on the fatigue performance in open-hole aluminum specimens. They carried out residual stress measurements, fractographic analysis, and numerical simulation. The results have shown presence of tensile residual stresses in the mid-section of the specimens after the treatment. Therefore, the positive effect of LSP was found when the hole was cut after the LSP and negative effect was encountered when the hole was already presented. P. Ouyang et al. [11] studied the effect of LSP on the fatigue life of Ti-6Al-4V titanium alloy experimentally and by means of numerical simulation. Numerical results have shown an improvement in the fatigue life of the peened specimen in more than 17 times in comparison with the non-treated one. However, experimental results haven't confirmed such significant enhancement. The authors explained that fact by the presence of local stress concentrators in the samples exposed by laser shots treatment which can cause a negative influence on the fatigue life. Zhao et al. [12] analyzed crack propagation rates for the CT-samples with a V-shape notch subjected to LSP with two different patterns obtained experimentally and by FEM simulation. They concluded that the considered LSP patterns (peening of the area near the notch root and peening of the area at some distance from the root) had led to a decrease in fatigue performance in comparison with the untreated sample. M. Achintha et al. [13] also concluded that laser shots treated open hole specimens can have low fatigue performance. They carried out fatigue tests on two aerospace-grade aluminum samples with two different thicknesses (thin and thick) and two different peening schemes as well as a numerical simulation of residual stress distribution in them. The experiments demonstrated some improvement in the fatigue life for thin specimens after LSP in the area around the hole and no effect for the thick ones. The numerical simulation explained these observations by the presence of tensile stresses in the mid-plane of the thick specimens.

In the present work, the influence of LSP patterns on the fatigue life of notched TC4 specimens is studied experimentally. Two LSP patterns different from each other by their location relative to the notch are used to form the residual stress

field in the notched area. The fatigue life of treated and untreated specimens is determined during fatigue tests. Numerical simulation of LSP allows us to visualize the created residual stress field and to interpret fatigue test results.

MATERIALS AND EXPERIMENTAL CONDITIONS

Titanium alloys are widely used in the aerospace industry and in engineering to produce structures, semi-finished products, and aircraft components. Alpha-beta titanium alloys are typically medium of high-strength materials (tensile strength ranging from 620 to 1250 MPa). However, their fatigue characteristics (fatigue life, fracture toughness, and so on) can be significantly improved by surface treatment processes such as LSP. In this work, specimens of TC4 (Ti-6Al-4V) titanium alloy with a semi-circular notch (Fig. 1) were investigated under fatigue loading conditions after laser shots treatment.

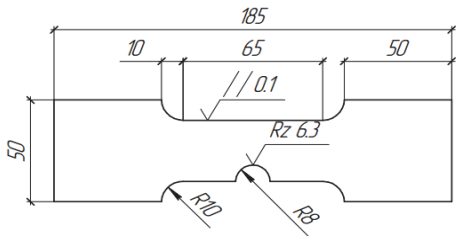

Figure 1: Geometry of studied specimens with the thickness of 3 mm (all dimensions are in millimeters).

LSP was carried out on the basis of the original Laser Pinning Complex assembled in the Institute of Continuous Media Mechanics of the Ural Branch of the Russian Academy of Sciences. It includes a Nd:YAG high energy laser Beamtech SGR-Extra-10, industrial robotic manipulator STEP SR50 and residual stress measurement system SINT MTS3000 RESTAN. Additional optic system can produce the laser beam with a square-form profile of 1 mm side. The pulse duration and energy of laser impact were 10 ns and 1 J, respectively. The aluminum foil of 80μm was used as an ablative layer. Two LSP patterns shown in Fig. 2 were realized.

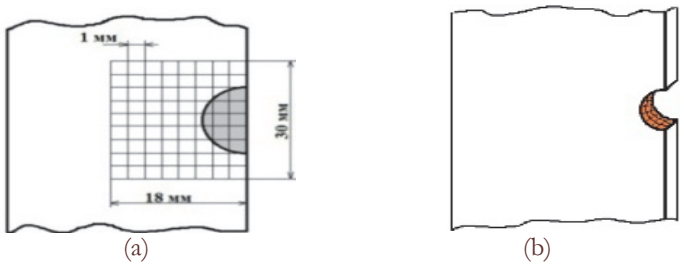

Figure 2: LSP pattern №1 (a) and LSP pattern №2 (b).

In the case of the LSP pattern №1 (Fig. 2 (a)), the treatment area was on the surface of the front and back side of specimen and includes the semi-circular notch zone. The LSP pattern №2 (Fig. 2 (b)) assumed the LSP treatment directly in semi-circular notch along a curved path. The laser beam was directed along the normal to the surface in both cases.
Two series of specimens treated by above mentioned two patterns were tested under uniaxial cyclic loading conditions. Fatigue experiments were carried out on a 100kN servo-hydraulic testing machine Bi-00-100 under constant maximum loading of 10 kN at a stress ratio R=0.1 and loading frequency 10 Hz. The number of cycles before fracture of specimens in two parts was registered for treated specimens and untreated ones (base material).

EXPERIMENTAL RESULTS

As a result of LSP, the residual stress field was formed on the specimen surface and under the surface up to a depth of 1 mm. The maximum value of compressive residual stress and the depth of its formation are the main characteristics that show the efficiency of laser shots treatment for the mechanical properties improvement. The

measurement of the residual stresses values versus the depth of the treated layer was carried out by the hole drilling method using an automatic system MTS3000-Restan (according to ASTM E837-13a). This method has a number disadvantages such as flat surface of the specimen, measurements only in one point of the surface, selection of suitable strain gauge sizes if specimen is small enough, providing only two components of residual stress and etc. Due to these restrictions, the drilling method allows us to measure the residual stress profile only in the case of the LSP pattern №1. A high curvature of the treated surface in the pattern №2 and its small size did not allow us to use the hole drilling method for residual stress profile determination. However, it is fair to assume that a laser impact of the same power density forms in the same material the residual stresses field with the similar magnitude and configuration. The dependence of residual stress components (σ_x, σ_y) on the subsurface layer depth (Fig. 3) was obtained for following characteristics of laser shot: 1 J energy impact, 10 ns pulse duration, 1 mm^2 beam profile area, 10GW/cm^2 power density.

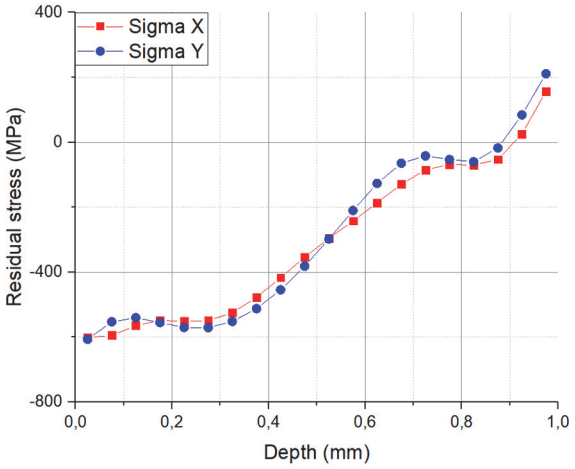

Figure 3: Residual stress components profile depends on layer depth.

Residual stress components σ_x and σ_y show approximately the same values at all depths. This indicates the isotropy of created residual stress on the surface. The maximum value of both compressive residual stress components is on the specimen surface and equal to 600 MPa approximately. The depth of the compressive residual stress field according to the graph in Fig. 3 is about 900 μm.

Results of fatigue test are presented in diagrams of Fig.4. They depict the dependence between number of cycles before fracture and specimen types (the base material, specimen treated by the LSP pattern №1, and specimen treated by the LSP pattern №2). After the fracture of the specimen, the number of cycles were taken as the fatigue life.

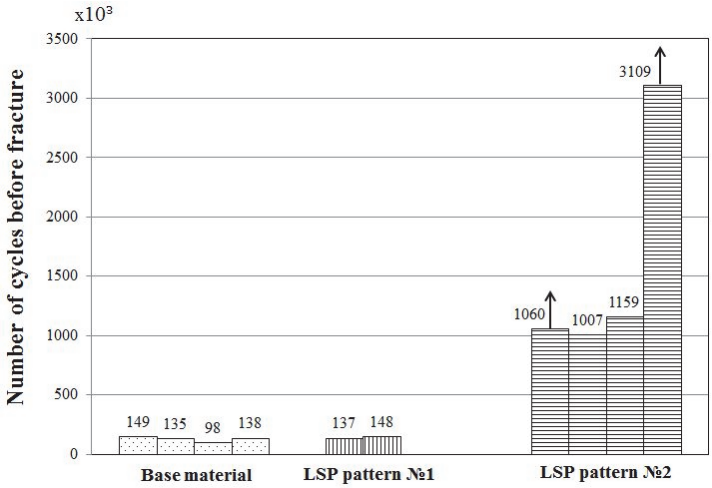

Figure 4: The number of cycles before failure during fatigue test of treated and untreated specimens (arrows indicate unbroken specimens).

According to the results of the fatigue test, the LSP pattern №1 doesn't have a significant influence on the fatigue life of the treated specimens. The average number of cycles before fracture of the base material and specimens treated by LSP pattern №1 is $130 \cdot 10^3$ cycles and $142 \cdot 10^3$ cycles, respectively. At the same time, the LSP pattern №2 induces a significant grow in the fatigue life (more than 10^6 cycles). Two specimens were broken near the grip (i.e. not in the treated semi-circular notched area). Another two specimens indicated by arrow in Fig.4 weren't broken at all. This experimental observation is probably related to the most optimal configuration of residual stress field generated by LSP in the stress concentrator region. In this case, the applied stress level, at which the fatigue crack grows in the base material, is not enough for a fatigue crack initiation in specimens after LSP by the pattern №2. To confirm this assumption, it is necessary to analyze the residual stress distribution in the stress concentrator region. Experimental measurements of residual stress distribution in this region are difficult. Therefore, to analyze the distribution of residual stresses in the specimen after the application of the LSP pattern №2 and explain the fatigue life improvement after LSP a numerical simulation has been carried out.

NUMERICAL SIMULATION

As it was shown above, LSP pattern № 1 didn't improve the fatigue life of the notched specimens. Similar results were obtained by other researchers [10, 13]. They obtained no improvement in the fatigue life of samples with stress concentrators. These results were related to the deteriorating effect of tensile residual stresses which occur in the specimen after the treatment. It was observed [10, 13] that tensile residual stresses produced in the mid-section of the specimen with stress concentrator during LSP of its front and rear sides contribute to negative effect on its fatigue performance. The LSP scheme № 2 is different and laser shots are applied directly at the concentrator. This peening pattern leads to a significant improvement in the fatigue performance of specimens. To analyze distribution of residual stresses in the sample after application of this pattern and explain these results the numerical simulation has been carried out. The numerical simulation was conducted using a finite-element model of a multi-shot LSP process which was developed in [14].

Finite-element model

In this work, only a brief description of the material model and numerical simulation process is given. More detailed information can be found in [14].

Similar to [15-19], LSP was considered as a purely mechanical process. Therefore, the formation of high-pressure plasma and surface ablation were neglected during the simulation. The effect of the laser pulse was taken into account by imposing mechanical pressure on the treated surface.

Numerical simulation was performed in finite-element software Abaqus. Fig. 5 shows the geometry of the computational domain. The geometry corresponds to the tested samples. Boundary conditions were assigned according to the experimental procedure. The half-circled zone near both ends of the gage at the front side (shaded areas at Fig. 5(a)) as well as half of the opposite side of the sample (without stress concentrator) (shaded area at Fig. 5(b)) were fixed. These conditions correspond to the gripping of the specimen by robotic arm in the LSP process.

The specimen was discretized by 8-node linear brick elements with reduced integration (C3D8R). A more refined mesh was applied at the peened area. Convergence study had shown that optimum size of the sample in this region was equal to 0.1 mm. In other regions mesh size was increased with the maximum element size which didn't exceed 2.5 mm.

The peening strategy was the same as in the LSP pattern № 2. Only the bore of the notch was subjected to LSP. The peening zone was a semicircular domain with chords at a distance of 4 mm from the external stress concentrator edges. Each laser shot was modeled by the two-step approach. The first step was dynamic which simulated elasto-plastic stress wave propagation induced by pulse loading. At this step, an explicit time integration scheme was applied. Laser pulse was imposed as a pressure boundary condition acting at the square region with an edge size of 1 mm of the stress concentrator surface. Following [16,20,21], it was assumed that pressure function for square spots is spatially homogeneous. A simple triangular approximation of dependence of the pressure P on time t was used as it has been proved to be valid for LSP simulation [15,22,23]:

$$P(t)=\begin{cases}\dfrac{t}{t_1}P_{peak}, & 0\le t<t_1,\\ \dfrac{t_2-t}{t_1}P_{peak}, & t_1\le t\le t_2\end{cases} \tag{1}$$

where t_1=2τ is the time of pressure increase, t_2=8τ is the time of pressure decrease, τ=10 ns is the laser pulse duration, P_{peak} is the peak pressure value. Parameters t_1 and t_2 for TC4 alloy were determined in our previous work [14] and verified for a large range of laser peak intensities from 3.3 GW/cm² to 40 GW/cm². The total duration of time at this step was equal to 10 μs to ensure that no further plastic strain had occurred.
Peak pressure was calculated according to Fabbro model of ablation in a confined medium [24]:

$$P_{peak}=0.01\sqrt{\frac{\alpha}{2\alpha+3}\cdot Z\cdot I} \tag{2}$$

where $Z=(2\cdot Z_{water}\cdot Z_t)/(Z_{water}+Z_t)$ is the combined acoustic impedance of water (Z_{water} = 0.17·106 g/(cm²··s)) and target (Z_t = 1.7·106 g/(cm²··s) for aluminum foil [25]), α is the efficiency coefficient which is typically equal to 0.33, I is the maximum energy density (10 GW/cm² in our case).
As the dynamic step had finished, the static step was calculated using an implicit time integration scheme. Stress tensor components, strain tensor components, and the displacement vector components were transferred from the previous (dynamic) step as the initial values for the static step. This step is aimed to simulate a stress-strain state after a laser shock impact. The stresses at the static equilibrium state are the residual stresses. This procedure was repeated for each shot until all stress concentrator area was peened.

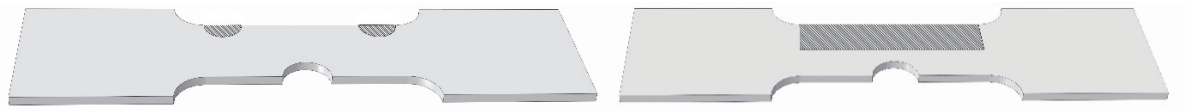

(a) (b)

Figure 5: Fixed boundary conditions: (a) front side, (b) rear side.

Material model

As LSP induces propagation of elasto-plastic waves in the material, the strain-rate sensitive model should be applied for its simulation. In our previous study [14] it has been shown that the Johnson-Cook plasticity model is effective for LSP modeling:

$$\sigma_{eq}=\left[A+B\left(\varepsilon_{eq}^{pl}\right)^{n}\right]\left[1+C\ln\frac{\dot{\varepsilon}_{eq}^{pl}}{\dot{\varepsilon}_0}\right] \tag{3}$$

where σ_{eq} is the equivalent stress, ε^{pl}_{eq} is the equivalent plastic strain, $\dot{\varepsilon}^{pl}_{eq}$ is the equivalent plastic strain rate, A is the yield stress, B is the strengthening coefficient, n is the strain hardening exponent, C defines strain-rate sensitivity, $\dot{\varepsilon}_0$ is the reference (quasistatic) stain rate. It should be noted that effects related to the thermal softening are negligible during LSP. Therefore, these effects are not considered in the present work [25-27].
Johnson-Cook material parameters and elastic constants for TC4 are presented in Tab. 1 [14]. The elastic material behavior was isotropic and described by Hook's law with two parameters (Young modulus and Poisson's ratio). Johnson-Cook material parameters were determined in [14] as a result of an identification procedure. Uniaxial stress-strain data obtained in the strain rate range from $5\cdot10^{-3}$ s^{-1} to $2.2\cdot10^{3}$ s^{-1} were used for this purpose. *A, B, n* parameters were defined using experimental quasistatic tensile diagram. Strain-sensitive material parameter *C* was obtained by dynamic stress-strain curves measured in a split-Hopkinson-bar testing system.

Parameter	Value	Unit	Symbol
Density	4424	kg/m^3	ϱ
Young's modulus	106.7	GPa	E
Poisson's ratio	0.314	-	ν
Quasi-static yield stress	978	MPa	A
Strengthening coefficient	826	MPa	B
Strain hardening exponent	0.639	-	n
Strain-sensitivity parameter	0.034	-	C
Reference strain rate	0.005	1/s	$\dot{\varepsilon}_0$

Table 1: Material parameters for TC4.

The above-described model was verified in [14] for a wide range of peak energy densities (from 3.3 GW/cm^2 to 40 GW/cm^2) and square spots with edge sizes varied from 1 mm to 3 mm. The verification was performed by comparison of the numerical in-depth residual stress profiles with the experimental data provided by the hole drilling method. The predicted results were in reasonable agreement with the experimental measurements for all considered cases.

Results of simulation

Fig. 6(a) shows the distribution of σ_{22} stress tensor component which is parallel to a longitudinal direction of the sample whose notch is subjected to the treatment with the LSP regime № 2. To present a more detailed distribution of residual stress near the stress concentrator, the results have been restricted by the cross sectional planes, one of which is located in the middle of the sample and the other one is at a distance of 1.25 cm from it. It can be seen that compressive residual stress is formed in the peening zone as expected. However, due to the complex geometry of the sample notch the distribution is non-homogeneous. The maximum compressive value is about -700 MPa and it is located in the middle of the stress concentrator surface. This part of the sample is the one where fatigue crack is expected to initiate. Therefore, it is important to produce compressive residual stress throughout the entire thickness of the sample and do not let the tensile stress within it. With the increase in the distance from the middle of the stress concentrator the compressive stress gradually declines. As the peening zone doesn't include the whole stress concentrator, compressive residual stress is absent in the area near the external edge of the concentrator. The figure shows that tensile stress in the middle part of the concentrator is located only under the peened surface and at the sample faces adjacent to the notch.

Fig. 6(b) illustrates the distribution of mechanical pressure, which gives us information about the mean value of three main stress tensor components. It can be seen that this value is also heterogeneous owing to the curvature of the stress concentrator. However, the maximum value of compressive residual stress is achieved along the whole peening zone. The location of tensile stress in the middle part of the concentrator is the same as for σ_{22}.

Fig. 6(c) presents the distribution of effective plastic strain after LSP with pattern №2. Due to the high curvature of the notch and the complex interaction between the residual stress generated by the first shots and elasto-plastic stress waves induced by each subsequent laser shot, the distribution of the plastic strain is non-homogenous. Only in the middle of the stress concentrator, a small zone with enough uniform strain distribution can be distinguished. On average, the magnitude of effective plastic strain is 1-3% which is explained by a high value of TC4 yield stress (Tab. 1).

On the whole, it can be seen that the LSP strategy №2 leads to favorable residual stress distribution. The tensile residual stress is located under the sample surface or in regions subjected to low loading during the fatigue test, while the highly loaded part of the sample under the fatigue test is surrounded by compressive residual stress.

To analyze the effect of the LSP pattern №2 on the stress state during uniaxial loading the peened sample was stretched with the maximum force applied in the fatigue experiment which was equal to 10 kN. Fig. 7 illustrates the distribution of σ_{22} stress tensor component over the whole sample. This component has been chosen as it is directed along the loading of the specimen. The tensile stress is localized in the middle part of the notch at the front surface. The same conclusion is valid for the opposite side of the specimen. The shape of the tensile zone is typical for this type of loading. The compressive residual stress is still can be seen at the inner surface of the stress concentrator.

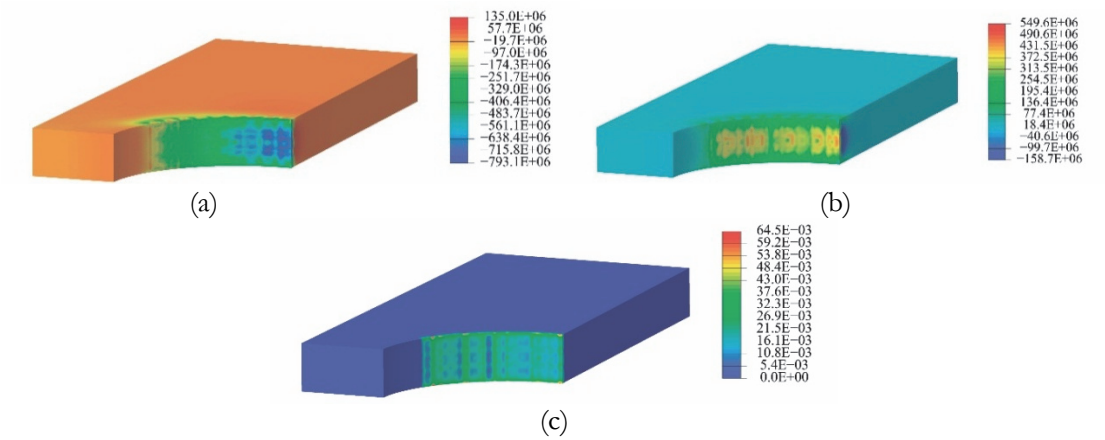

Figure 6: Distribution of (a) σ_{22} stress tensor component, (b) pressure, (c) effective plastic strain along the part of the sample restricted by two vertical planes (the first one located at the middle of the sample and the second one is at the distance of 1.25 cm from it) after LSP.

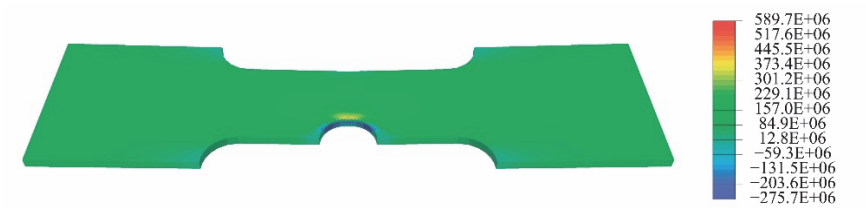

Figure 7: Distribution of σ_{22} stress tensor component (along the loading direction) after tension with the loading equal to 10 kN.

For the detailed analysis of the stress state near the notch, the same part of the specimen as in Fig. 6 has been chosen. Fig. 8(a) presents the distribution of σ_{22}. The maximum tensile stress is still under the surface of the sample. However, the compressive residual stress near the edges of the notch converts into tensile. Also, the value of compressive residual stress in the middle part of the notch surface diminishes due to the tensile loading. The compressive residual stress becomes more homogeneous near the chords bounding the peening zone. This part is less loaded than the middle part of the sample under mode I loading.

Fig. 8(b) illustrates mechanical pressure distribution in the sample after the loading. A similar pattern as for σ_{22} can be observed. The zones of maximum compressive stress are located near the bounding chords of the peening area. The tensile zones aroused under the surface and near the edges of the stress concentrator.

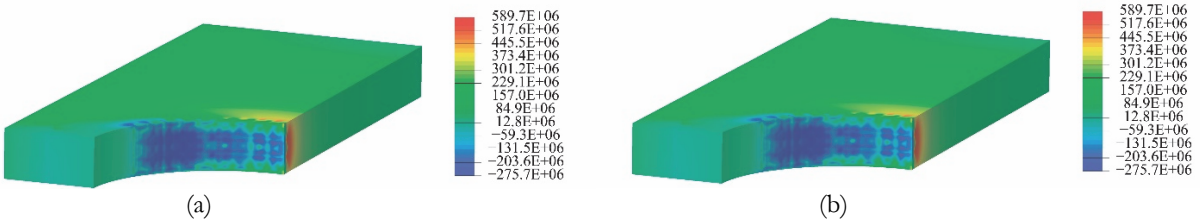

Figure 8: Distribution of (a) σ_{22} stress tensor component (along the loading direction) and (b) pressure along the part of the sample restricted by two vertical planes (the first one located at the middle of the sample and the second one is at the distance of 1.25 cm from it) after tension with the loading equal to 10 kN.

Fig. 9 gives results in a more suitable for comparison purposes way. Fig. 9(a) presents profiles of residual stresses induced by LSP pattern №2 along the specimen thickness at the three different positions of the notch surface. The first curve is located in the middle of the notch, the second curve is at the quarter of the notch radius, and the third curve is near the chord of the peening zone. All curves show that there is a compressive stress state at the surface of the notch after LSP.

The values near the edges of the notch are lower than values at the middle of the thickness. As it was mentioned above, the maximum compressive residual stress is observed in the middle part of the notch. For the considered location of the curve, its value is -700 MPa. With the increase in the distance from the center, the compressive stress declines. At the quarter of the notch radius, its absolute value decreases by 1.6 times and is about -430 MPa. The lowest value is near the boundary of the peening zone and it is equal to -160 MPa. Fig. 9(b) shows profiles of σ_{22} stress tensor component in the peened specimen subjected to tension. The profiles are obtained for the same locations as in Fig. 9(a). The significant increase in the σ_{22} for the first and the second curve can be observed. For the third curve the results are nearly the same as after LSP pattern №2 without any loading. This indicates that this zone is only slightly affected by the loading. Due to the rise in stress all curves have similar values which varies from -230 MPa to -150 MPa for the thickness interval from 1 to 2 mm. However, the second curve demonstrates that the stress level near the front and rear faces of the sample is close to zero. Moreover, the third profile indicates tensile stress state of the sample near the boundary chord of the peening zone.

The minimum value of the stress component in the middle of the notch shown by the first profile is equal to -150 MPa (Fig. 9(b)). Therefore, the external loading induces a decline in compressive stress in this region about 4.7 times in comparison with the unloaded case (Fig. 9(a)). Nevertheless, the stress state in the notch remains compressive. Although the tensile stress occurs in the other two considered regions due to the external loading, its maximum value at the surface does not exceed 300 MPa which is significantly lower than the yield stress of TC4 alloy (Tab. 1). Consequently, during cyclic loading, the sample in the notch area undergoes only elastic deformation. Thus, the LSP pattern №2 leads to the improvement in the fatigue life observed in the test, as the largest tensile stress is located only under the peened surface as it is shown in Fig. 9.

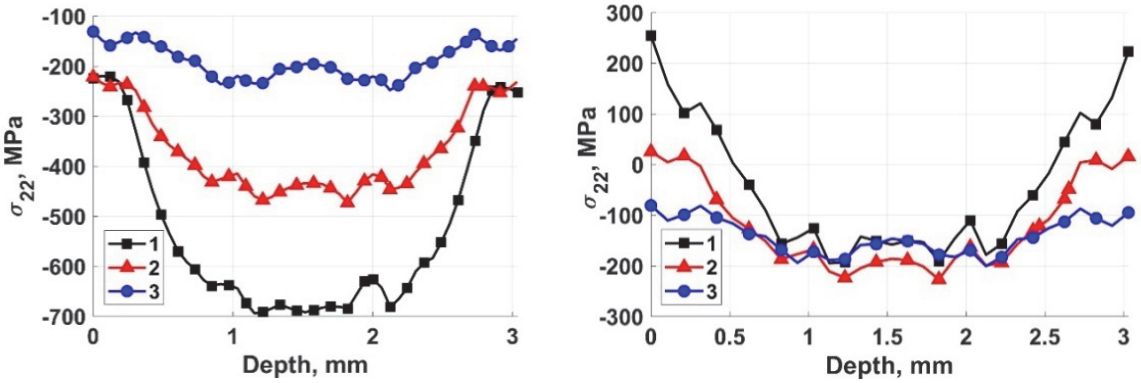

Figure 9: σ_{22} stress tensor component at the surface of stress concentrator vs width of the sample: (a) after LSP, (b) after tension with the loading equal to 10 kN (1 – line located at the middle of the LSP zone, 2 – line located near the edge of LSP zone, 3 – line located at the quarter of LSP zone).

The effect of tensile loading on the subsurface distribution of stress is illustrated in Fig 10. The results present the profile of σ_{22} stress tensor component along the middle line passing through the width of the specimen. This line starts at the notch root in the middle depth of the sample and ends at a distance of 2.3 mm from it. The figure compares two cases. The first line corresponds to the residual stress after pattern №2 in the absence of the external loading. The second line shows the stress profile in the peened sample after the tension of it with a force equal to 10 kN. From the first curve, it can be seen that the penetration depth of the compressive residual stress after LSP pattern №2 is about 0.6 mm. The minimum value is around -700 MPa similar to the Fig. 9(a). The maximum tensile stress is at the depth of 0.9 mm and it is equal to 90 MPa. The difference in minimum value of residual stress between experimental results presented in Fig. 3 and numerical results given in Fig. 10 is nearly 16%. This minor disagreement can be explained by possible measurement inaccuracies of the incremental hole drilling method due to its incremental and destructive character. Difference in the penetration depth of compressive residual stresses is explained by the different conditions of elastic-plastic stress wave propagation. Experimental results presented in Fig. 3 correspond to the LSP pattern №1, where the plane surface of the sample has been treated, while numerical results given in Fig. 10 correspond to the LSP pattern №2, where curvilinear surface of the stress concentrator has been peened. It should be noted also that numerical results demonstrate the effect of stress drop on the peened surface. It can be seen that the maximum value of compressive stress is observed not at the material surface, but in the near-surface zone. This effect is associated with the generation of surface relaxation waves

from the perimeter of the laser spot, which results in a decrease of compressive stresses at the treated surface [28-30]. A specific feature of the hole drilling method is the averaging of the obtained data over the drilled area. Therefore, it can affect the ability of it to register properly the above-described effect.

After the tension the stress component increases (the second curve in Fig. 10). The minimum value becomes equal to -180 MPa which indicates the substantial effect of the loading though at the notch surface stress is still compressive. At the same time, the penetration depth of compressive stress is declined by 60% and has a value of 0.2 mm. The maximum subsurface tensile stress is at the same depth and is around 500 MPa which is 5.5 times higher than after LSP pattern №2. Despite the fact, that there is a substantial increase in subsurface tensile stress this value is also lower than the yield stress of TC4. Thus, it can be concluded that LSP regime №2 is effective because it contributes to the decrease in the stress value in the highly-loaded regions of the sample.

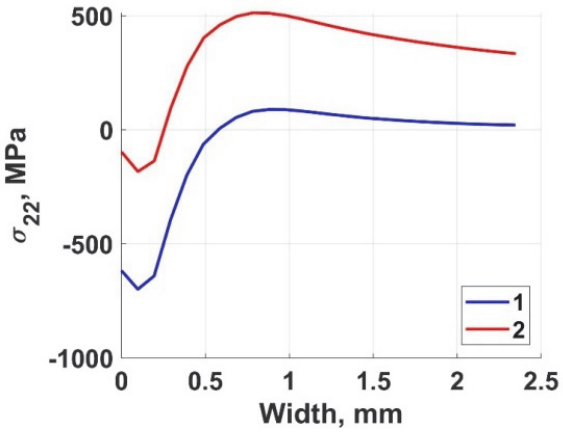

Figure 10: σ_{22} stress tensor component along the middle line passing through the width of the sample (1 – after LSP, 2 – after tension with the loading equal to 10 kN)

Conclusions

The work presented experimental results on the fatigue life of the notched TC4 specimens subjected to LSP. Two LSP patterns were examined in the context of fatigue life improvement. The experimental study has shown that different LSP schemes with the same characteristics of laser impact have a discrepant effect on the fatigue life. An important role is played not only by laser impact characteristics but also configuration and place of LSP of sample surface relative to the stress concentrator region and loading conditions. In the present case, it has been found that LSP of the stress concentrator area leads to a more significant improvement of fatigue properties of the sample in comparison with the conventional approach when the front and rear surfaces of the sample near the notch are peened. The proposed LSP pattern increases the fatigue life of specimens with a semi-circular notch by an order of magnitude. The numerical simulation of the LSP regime was performed to visualize the residual stress field in the treated specimen after loading and to give the interpretation of the experimentally observed improvement of the fatigue life. The applied LSP model was based on a two-step approach according to which dynamic and static problems were solved to obtain residual stress distribution after each shot. Although this method is characterized by substantial computational costs, it provides an accurate representation of the residual stress field. The numerical results have shown that the chosen treatment regime let us avoid the formation of the tensile stress at the middle section of the sample notch. Since the tensile stress increases during subsequent fatigue test and causes a crack initiation, reduction of it due to LSP contributes to the fatigue life improvement. When the semi-circular notch of the sample is subjected to LSP, the bore of the notch is in compressive stress state and the maximum tensile residual stress is located under the surface of the sample. Subsequent tension of the sample with the loading corresponding to the maximum force in the fatigue experiment induces decrease in the compressive stress in the middle part of the stress concentrator as well as the rise in the tensile stress inside the sample. However, the surface tensile stress is far from the yield stress and the specimen deforms in the elastic range during fatigue loading. Therefore, the substantial improvement in fatigue life is observed in the experiment.

ACKNOWLEDGMENTS

Experimental part of work concerning examination of laser shock peening patterns and fatigue tests of titanium alloys TC4 (Вт6 in Russia) specimens was supported by RSF (project No. 22-79-10168). Numerical simulations of laser shock peening were supported by the Government of Perm Krai, research project No. C-26/829.

REFERENCES

[1] Sanchez, A. G., Leering, M., Glaser, D., Furfari, D., Fitzpatrick, M. E., Wharton, J. A. and Reed, P. A. S. (2021). Effects of ablative and non-ablative laser shock peening on AA7075-T651 corrosion and fatigue performance, Materials Science and Technology, 37(12), pp. 1015-1034. DOI: 10.1080/02670836.2021.1972272.

[2] Pretorius, J.G., Desai, D.A., Snedden, G.C. (2019). Effect of Laser Shock Peening on Fatigue Life at Stress Raiser Regions of a High-Speed Micro Gas Turbine Shaft: A Simulation Based Study, International Journal of Engineering Research in Africa, 45, pp. 15-27. DOI: 10.4028/www.scientific.net/JERA.45.15.

[3] Ren, X., Chen, B., Jiao, J., Yang, Y., Zhou, W. and Tong, Z. (2020). Fatigue behavior of double-sided laser shock peened Ti-6Al-4V thin blade subjected to foreign object damage, Opt. Laser Technol., 121, p. 105784. DOI: 10.1016/j.optlastec.2019.105784.

[4] Yang, J.-M., Her, Y.C., Han, N., Clauer, A. (2001). Laser shock peening on fatigue behavior of 2024-T3 Al alloy with fastener holes and stopholes, Sci Eng., A298(296), p. 9.

[5] Kaufman, J., Špirit, Z., Vasudevan, V.K., Steiner, M.A., Mannava, S.R., Brajer, J., Pína, L., Mocek, T. (2021). Effect of Laser Shock Peening Parameters on Residual Stresses and Corrosion Fatigue of AA5083, Metals, 11, p. 1635. DOI: 10.3390/met11101635.

[6] Clauer, A.H. (1996). Laser Shock Peening for Fatigue Resistance, In: Surface Performance of Titanium, TMS, pp. 271–230.

[7] Liu, K.K., Hill, M.R. (2009). The effects of laser peening and shot peening on fretting fatigue in Ti–6Al–4V coupons, Tribology International, 42, pp. 1250–1262.

[8] Epp, J., Zoch, H.-W. (2016). Comparison of Alternative Peening Methods for the Improvement of Fatigue Properties of Case-Hardened Steel Parts, J. Heat Treatm. Mat., 71, p. 3.

[9] Ali, A-J. H. (2016). Improvement of fatigue life of aa 7075 using laser shock peening (lsp) surface treatment technique, AL- Taqani , 29 (1), pp. 47-54.

[10] Ivetic, G., Meneghin, I., Troiani, E., Molinari, G., Ocaña, J., Morales, M., Porro, J., Lanciotti, A., Ristori, V., Polese, C., Plaisier, J., Lausi, A. (2012). Fatigue in laser shock peened open-hole thin aluminium specimens, Materials Science and Engineering: A, 534, pp. 573-579.

[11] Ouyang, P., Luo, X., Dong, Z., Zhang, S. (2022). Numerical Prediction of the Effect of Laser Shock Peening on Residual Stress and Fatigue Life of Ti-6Al-4V Titanium Alloy, Materials, 15, p. 5503. DOI: 10.3390/ma15165503.

[12] Zhao, J., Dong, Y., Ye, C. (2017). Laser shock peening induced residual stresses and the effect on crack propagation behavior, International Journal of Fatigue, 100, pp. 407-417. DOI: 10.1016/j.ijfatigue.2017.04.002.

[13] Achintha, M., Nowell, D., Fufari, D., Sackett, E.E., Bache, M.R. (2014). Fatigue behaviour of geometric features subjected to laser shock peening: Experiments and modeling, International Journal of Fatigue, 62, pp. 171–179. DOI: 10.1016/j.ijfatigue.2013.04.016

[14] Kostina, A., Zhelnin, M., Gachegova, E., Prokhorov, A., Vshivkov, A., Plekhov, O. and Swaroop, S. (2022). Finite-element study of residual stress distribution in Ti-6Al-4V alloy treated by laser shock peening with varying parameters, Frattura ed Integrità Strutturale, 16(61), pp. 419–436. DOI: 10.3221/IGF-ESIS.61.28

[15] Braisted, W., Brockman, R. (1999). Finite element simulation of laser shock peening, Int. J. Fatigue, 21, pp. 719-724. DOI: 10.1016/S0142-1123(99)00035-3

[16] Keller, S., Chupakhin, S., Staron, P., Maawad, E., Kashaev, N., Klusemann, B. (2018). Experimental and numerical investigation of residual stresses in laser shock peened AA2198, J. Mater. Process. Technol., 255, pp. 294-307. DOI: 10.1016/j.jmatprotec.2017.11.023

[17] Hfaiedh, N., Peyre, P., Song, H., Popa, I., Ji, V. (2015). Finite element analysis of laser shock peening of 2050-T8 aluminum alloy, Int. J. Fatigue, 70, pp. 480-489. https://doi.org/10.1016/j.ijfatigue.2014.05.015

[18] Zhang, X., Li, H., Duan, S., Yu, X., Feng, J., Wang, B., Huang, Z. (2015). Modeling of residual stress field induced in Ti–6Al–4V alloy plate by two sided laser shock processing, Surf. Coat. Technol., 280, pp. 163-173. DOI: 10.1016/j.surfcoat.2015.09.004,

[19] Kim, R., Suh, J., Shin, D., Lee, K.-H., Bae, S.-H., Cho, D.-W., Yi, W.-G. (2021). FE Analysis of laser shock peening on STS304 and the effect of static damping on the solution, Metals, 11, p. 1516. DOI: 10.3390/met11101516,

[20] Xu, G., Luo, K. Y., Dai, F. Z. and Lu, J.Z. (2019). Effects of scanning path and overlapping rate on residual stress of 316L stainless steel blade subjected to massive laser shock peening treatment with square spots, Appl. Surf. Sci., 481, pp. 1053-1063. DOI: 10.1016/j.apsusc.2019.03.093

[21] Hu, Y., Gong, C., Yao, Z. and Hu, J. (2009). Investigation on the non-homogeneity of residual stress field induced by laser shock peening, Surf. Coat. Technol., 203, pp. 3503-3508. DOI: 10.1016/j.surfcoat.2009.04.029

[22] Wang, C., Li, K., Hu, X., Yang, H. and Zhou, Y. (2021). Numerical study on laser shock peening of TC4 titanium alloy based on the plate and blade model, Opt. Laser Technol., 142, p. 107163. DOI: 10.1016/j.optlastec.2021.107163

[23] Li, X., He, W., Luo, S., Nie, X., Tian, L., Feng, X. and Li, R. (2019). Simulation and experimental study on residual stress distribution in titanium alloy treated by laser shock peening with flat-top and Gaussian laser beams, Materials, 12, p. 1343. DOI: 10.3390/ma12081343

[24] Fabbro, R., Fournier, J., Ballard, P., Devaux, D. and Virmont, J. (1990). Physical study of laser-produced plasma in confined geometry, J. Appl. Phys., 68, pp. 775-784. DOI: 10.1063/1.346783

[25] Langer, K. and Spradlin, T.J, Fitzpatrick, M. E. (2020). Finite element analysis of laser peening of thin aluminum structures, Metals, 10, p. 93. DOI:10.3390/met10010093

[26] Sticchi, M., Staron, P., Sano, Y., Meixer, M., Klaus, M., Rebelo-Kornmeier, J., Huber, N., Kashaev, N. (2015). A parametric study of laser spot size and coverage on the laser shock peening induced residual stress in thin aluminium samples, J. Eng., 2015, pp.1-9. DOI: 10.1049/joe.2015.0106

[27] Spradlin, T.J., Grandhi, R.V., Langer, K. (2011). Experimental validation of simulated fatigue life estimates in laser-peened aluminum, Int. J. Struct. Integr., 2, pp. 74–86.

[28] Zhang, X., Li, H., Duan, S., Yu, X., Feng, J., Wang, B., Huang, Z. (2015). Modeling of residual stress field induced in Ti–6Al–4V alloy plate by two sided laser shock processing, Surf. Coat. Technol., 280, pp. 163-173. DOI: 10.1016/j.surfcoat.2015.09.004

[29] Xu, G., Luo, K. Y., Dai, F. Z., Lu, J. Z. (2019). Effects of scanning path and overlapping rate on residual stress of 316L stainless steel blade subjected to massive laser shock peening treatment with square spots, Appl. Surf. Sci., 481, pp. 1053-1063.DOI: 10.1016/j.apsusc.2019.03.093.

[30] Hu, Y., Gong, C., Yao, Z., Hu, J. (2009). Investigation on the non-homogeneity of residual stress field induced by laser shock peening, Surf. Coat. Technol., 203, pp. 3503-3508. DOI: 10.1016/j.surfcoat.2009.04.029.